Optics Letters

Dispersion of coupled mode-gap cavities

JIN LIAN,[1,*] SERGEI SOKOLOV,[1] EMRE YÜCE,[1] SYLVAIN COMBRIÉ,[2] ALFREDO DE ROSSI,[2] AND ALLARD P. MOSK[1]

[1]Complex Photonic Systems (COPS), MESA+ Institute for Nanotechnology, University of Twente, P.O. Box 217, 7500 AE Enschede, The Netherlands
[2]Thales Research and Technology, Route Départementale 128, 91767 Palaiseau, France
*Corresponding author: j.lian@utwente.nl

Received 29 June 2015; revised 26 August 2015; accepted 26 August 2015; posted 27 August 2015 (Doc. ID 243898); published 28 September 2015

The dispersion of a coupled resonator optical waveguide made of photonic crystal mode-gap cavities is pronouncedly asymmetric. This asymmetry cannot be explained by the standard tight binding model. We show that the fundamental cause of the asymmetric dispersion is the inherent dispersive cavity mode profile; i.e., the mode wave function depends on the driving frequency, not the eigenfrequency. This occurs because the photonic crystal cavity resonances do not form a complete set. We formulate a dispersive mode coupling model that accurately describes the asymmetric dispersion without introducing any new free parameters.

OCIS codes: (130.5296) Photonic crystal waveguides; (140.3945) Microcavities.

http://dx.doi.org/10.1364/OL.40.004488

In coupled cavity systems in photonic crystals (PhC), light transport occurs via evanescent field coupling between high-quality factor (Q) cavities. The well-known example is the coupled resonator optical waveguide (CROW), which is a linear chain of cavities [1]. Arrays of coupled cavities have attracted substantial scientific attention for practical applications, such as slow light engineering and strong light–matter interaction enhancement [2–4], and many novel phenomena of fundamental interest, such as gauge fields [5,6] and time-reversal of light pulses [7,8].

Realizations of low loss and compact CROWs require high-Q, wavelength-sized cavities. Mode-gap cavities [9] created by shifting some of the holes around PhC waveguides as shown in Fig. 1(a) have been demonstrated to be extremely suitable for creating large-scale cavity arrays [10,11].

The tight binding (TB) model [1,12] is the usual approach for modeling the dispersion in coupled cavities [3,4,13,14]. The core concept of the TB model is that in coupled cavities the wave functions are tightly confined in each cavity. The eigenmodes of the individual cavities are then coupled to yield waveguide modes. Coupling between neighboring cavities is due to the overlap of the eigen wave function of the cavity modes. The dispersion of the CROW band as predicted by the TB model is a cosine curve [1]. For a given structure, its parameters can be evaluated by numerical methods, such as plane wave expansion (PWE) [15] and finite-difference time-domain (FDTD) [16].

However, the TB model does not describe the dispersion of a CROW composed of mode-gap cavities correctly. In Fig. 1(b), we show the group velocity curve as obtained from the TB model and as calculated by FDTD [17]. The TB result is perfectly symmetric with respect to $k = 0.5\pi/R$. In contrast, the FDTD result is pronouncedly asymmetric. The asymmetric spectrum has also been observed experimentally [11]. It is remarkable that the TB model fails here, as it depends only on the assumption of energy-independent eigenmodes, which

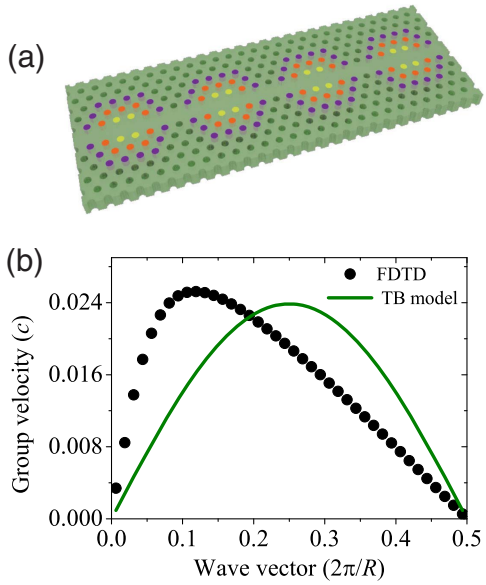

Fig. 1. (a) Schematic of a CROW composed of coupled mode-gap cavities. The cavities are created by shifting the yellow, red, and purple holes around the waveguide in a tapered way. The width of the waveguide is $0.98\sqrt{3}a$ (a is the lattice constant). The radius of the holes is $0.25a$. The shift of the yellow holes is S1 $= \eta 0.0124\sqrt{3}a$, where η is a factor we call modulation strength. The shifts of the red and purple holes are 2/3 S1 and 1/3 S1, respectively. (b) Group velocity of the 2D CROW consisting of mode-gap cavities with modulation strength 1.5 calculated by 2D FDTD (black dots) and TB model (green line). Parameters are calculated by FDTD.

is a direct consequence of the completeness of the set of eigenmodes [18].

In this Letter, we uncover the physical origin of the discrepancy and propose an improved mode coupling model.

The resonant modes of a closed conservative cavity form a complete set. An important consequence of completeness is the fact that the response of a cavity is defined in terms of modes that do not depend on the driving frequency themselves. In an open cavity, we have quasi-modes, which form a complete set only if certain conditions are fulfilled [19]; essentially, the edge of the resonant mode must be clearly defined in the structure and no outgoing waves should be scattered back to the cavity. These conditions are never fulfilled in a PhC cavity. In a PhC cavity, light is confined by constructive interference of Bragg reflection, and the Bragg reflection takes place throughout the PhC structure. As a result, the quasi-modes do not form a complete set and their spatial profile depends on the driving frequency; i.e., the mode profile is dispersive.

The breakdown of completeness for an open cavity shows a signature in driven oscillation. If the cavity is driven at frequency ω, the field inside the cavity will be $\mathbf{E}(\mathbf{r}, t) = \mathbf{E}(\mathbf{r}, \omega) \exp(-i\omega t)$, where $\mathbf{E}(\mathbf{r}, \omega) \neq \mathbf{E}(\mathbf{r}, \omega_0)$. Alternatively speaking, when an open cavity is driven, the wave function of the mode is determined by the driving frequency, not the free oscillation frequency.

In CROWs, therefore, the coupling between neighboring cavities is not characterized by the overlap of the eigenmodes of the single cavity $\mathbf{E}(\mathbf{r}, \omega_0)$ (ω_0 is the eigenfrequency of the cavity) but of the dispersive modes $\mathbf{E}(\mathbf{r}, \omega)$.

In Fig. 2, the dispersion of a quasi-mode is shown qualitatively. In a true eigenmode, the size of the mode profile should always be the same as the cavity is driven at different frequencies. However, the quasi-mode is dispersive and is spatially narrower [Fig. 2(a)] or wider [Fig. 2(b)] than the free oscillation mode when the driving frequency is lower or higher than the intrinsic frequency, respectively.

We performed two-dimensional (2D) FDTD simulations to quantitatively study the dispersion of the mode profile of PhC mode-gap cavities. In the simulation, a continuous source was placed in the center of a single cavity and switched on smoothly. After the transient died out, we output the E_y field across the waveguide direction. The same procedure was repeated several times at different frequencies and different cavities [20].

In Fig. 3(a), we plot the amplitudes of the E_y field versus the position across the waveguide direction when we drive the cavity at three different frequencies. When the driving frequency is $\omega_0 + \delta_1$, which is higher than the resonant frequency ω_0, the

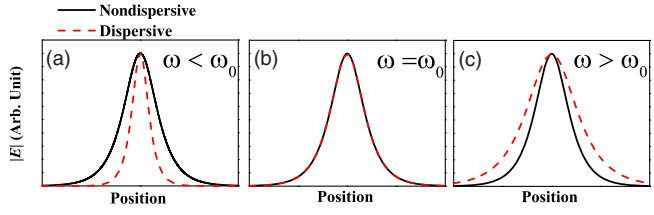

Fig. 2. In driven oscillation, the quasi-mode (red) will be (a) smaller or (c) larger compared to the intrinsic resonant mode in the case in which the driving frequency is lower or higher than the intrinsic frequency. In contrast, a true eigenmode (black) keeps the same spatial profile when driven off-resonance.

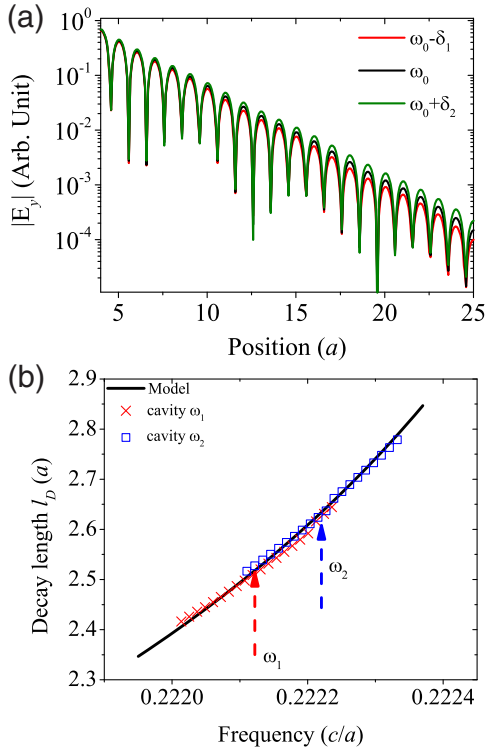

Fig. 3. (a) 2D FDTD simulation of forced driven oscillation of a mode-gap cavity. The amplitude of the E_y field across the waveguide direction versus the position is plotted. The center position is located at 0. The red, black, and green lines illustrate cases with different driving frequencies ($\omega_0 = 0.22212c/a$, $\delta_1 = 0.00011c/a$, and $\delta_2 = 0.00010c/a$). (b) Red crosses (blue squares) depict decay lengths of a cavity with intrinsic frequency $\omega_1 = 0.22212c/a$ ($\omega_2 = 0.22222c/a$). The black curve is the model we use to describe the decay length. The decay lengths are obtained by fitting the envelope of the field from $x = 4a$ to $x = 14a$. The only difference between the geometries of the two cavities is the modulation strength.

decay in space is slower. Alternatively speaking, the mode is larger in space. When the driving frequency is $\omega_0 - \delta_2$, the mode is smaller. This clearly shows that for a single mode-gap cavity, the mode profile differs depending on the driving frequency. Outside the modulation part of the cavity, the envelope of the mode profile decays exponentially. Along the waveguide direction x, the envelope decays as $\exp(-x/l_D)$, where l_D is the decay length and $x = 0$ is the center of the cavity. The decay length is related to the dispersion of the waveguide where the cavity lies in. The waveguide dispersion above the bandedge can be expanded as $\omega = \omega_{\text{edge}} + (k - \pi/a)^2/(2m)$ [21], where $m = (\partial^2\omega/\partial^2 k)^{-1}$ is the photon mass in analogy to the effective mass of electrons [12] and ω_{edge} is the frequency of the edge of the waveguide band. By analytic continuation of the dispersion, the wave vector k becomes a complex number when $\omega < \omega_{\text{edge}}$. The decay length, which is the inverse of the imaginary part of the wave vector, follows as $l_D = (2m(\omega_{\text{edge}} - \omega))^{-1/2}$. In Fig. 3(b), we plot the calculated decay lengths by the analytical model and the extracted decay lengths from FDTD simulations of two different cavities at various driving frequencies. First, we see that when the cavity is driven at different frequencies, the decay lengths differ. Second, for two different cavities (one with intrinsic frequency ω_1 and the other with

intrinsic frequency ω_2), when the driving frequencies are the same, the decay lengths are the same. The decay lengths are well described by the analytical model, and we conclude that mode-gap cavities have a mode profile that depends on the driving frequency, not the resonant frequency.

As the consequence of the dispersive mode profile, the mode functions in the expression of the coupling rate [1,22] should be the dispersive mode (DM), not the eigenmode. The expression of the coupling rate becomes

$$\Gamma(\omega) = \frac{\omega \int \delta\epsilon(\mathbf{r}-\mathbf{R})\mathbf{E}_\omega(\mathbf{r}-\mathbf{R})\cdot\mathbf{E}_\omega(\mathbf{r})\mathrm{d}\mathbf{r}}{\int \epsilon(\mathbf{r})\mathbf{E}_\omega(\mathbf{r})\cdot\mathbf{E}_\omega(\mathbf{r})\mathrm{d}\mathbf{r}}. \quad (1)$$

In Eq. (1), $\mathbf{E}_\omega(\mathbf{r})$ is the electric field of the wave function at frequency ω, $\epsilon(\mathbf{r})$ is the dielectric constant of a single cavity, and $\delta\epsilon(\mathbf{r}-\mathbf{R})$ is the dielectric difference between one isolated cavity and two cavities with heart-to-heart distance $\mathbf{R}$. This expression is identical to that derived by Haus and Huang [22] and Yariv *et al.* [1], except for the replacement of the resonant mode profile $\mathbf{E}_{\omega_0}(\mathbf{r})$ by the dispersive mode profile $\mathbf{E}_\omega(\mathbf{r})$. The resulting dispersion of the CROW is

$$\omega = \omega_0 + \Delta + \Gamma(\omega)\cos(kR), \quad (2)$$

where ω_0 is the eigenfrequency of the single resonators and Δ is the frequency difference between ω_0 and the center of the CROW band.

To evaluate Eqs. (1) and (2), some assumptions are made. First, we assume that each polarization of $\mathbf{E}_\omega(\mathbf{r})$ can be decomposed into $E^X_\omega(x)E^{YZ}_\omega(y,z)$. Here, x and y represent the spatial coordinates, and x is along the waveguide direction, where $E^{YZ}_\omega(yz)$ can be approximated to be nondispersive, $E^{YZ}_\omega(y,z) \approx E^{YZ}_{\omega_0}(y,z)$. Second, we approximate the envelope of $E^X_\omega(x)$ by $1/\cosh(x/l_D)$, which is a reasonable approximation for mode-gap cavities. The last assumption is for $\delta\epsilon(\mathbf{r}-\mathbf{R})$ and $\epsilon(\mathbf{r})$. We divide $\delta\epsilon(\mathbf{r}-\mathbf{R})$ into five blocks. For each block, the effects of $\delta\epsilon$ are essentially the increase of the effective dielectric function of the waveguide. We approximate that this increase happens at the center of each block, so we express $\delta\epsilon$ as a collection of delta functions $\delta\epsilon = \sum_{j=-2}^{2}\delta(x-x_j)\bar{\delta}\epsilon_j$ with $x_j = ja$ and $\bar{\delta}\epsilon_j = \frac{3-|j|}{3}\bar{\delta}\epsilon_0$ (where $\bar{\delta}\epsilon_0$ is a constant). Based on these three assumptions, the coupling rate is

$$\Gamma(\omega) = \beta\sum_{j=-2}^{2}\frac{(3-|j|)\omega}{l_D\cosh\left(\frac{R-ja}{l_D}\right)\cosh\left(\frac{ja}{l_D}\right)}. \quad (3)$$

Here, β is a proportionality constant resulting from the integral over y, and we may abbreviate $\Gamma(\omega) = \beta g(\omega)$, where we emphasize that $g(\omega)$ can be evaluated analytically. The dispersion relation becomes

$$\omega = \omega_0 + \Delta + \beta g(\omega)\cos(kR). \quad (4)$$

There are only three unknowns (ω, Δ, β), which is exactly the same number of unknowns that the TB model has; i.e., our model does not introduce any extra free parameters.

We show the normalized coupling rate of the CROW structure in Fig. 1 as a function of normalized frequency detuning $\delta = (\omega-\omega_0)/\Gamma_0$ with $\Gamma_0 = \Gamma(\omega_0)$ in Fig. 4. The normalized coupling rate is defined as $\Gamma(\omega)/\Gamma_0$; it is also equivalent to $g(\omega)/g(\omega_0)$. The normalized coupling rate in Fig. 4 increases nonlinearly as the detuning increases; in other words, $\Gamma(\omega)$ is highly dispersive. At the low k values, which correspond to positive detuning δ, the coupling rate is larger, and therefore the group velocity is enhanced. As a result, the maximum of the group velocity shifts to low k values as compared to the result from the TB model.

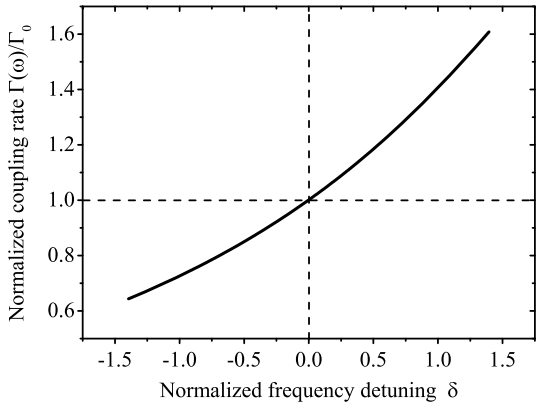

Fig. 4. Normalized coupling rate $\Gamma(\omega)/\Gamma_0$ of the CROW structure in Fig. 1 versus the normalized frequency detuning δ.

We present the calculated group velocity of the CROW in 2D and in a 3D membrane structure in Fig. 5. In Fig. 5(a), the results of group velocity calculated by the DM model are asymmetric with a maximum at $k \approx 0.10\ (2\pi/R)$; this matches the 2D FDTD results extremely well. In Fig. 5(b), the group velocity from the DM model is asymmetric with maximum at

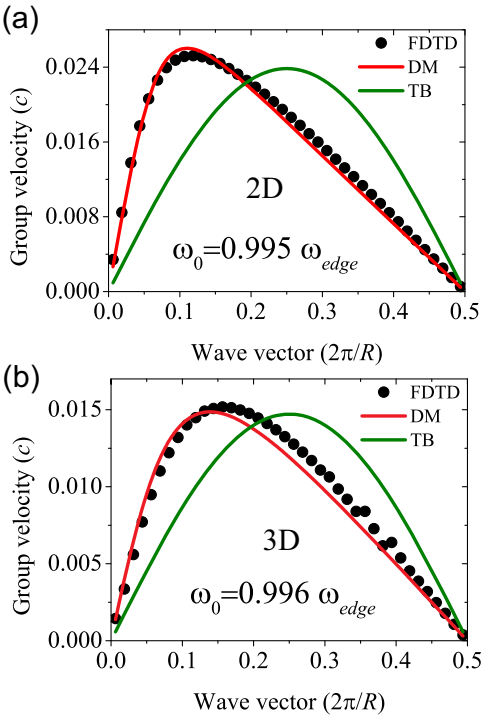

Fig. 5. (a) Group velocity of the 2D CROW consisting of mode-gap cavities with modulation strength 1.5 calculated by FDTD (black dots), TB model (green line), and DM model (red line). All the parameters are the same as those in simulations of driven oscillation. (b) Group velocity of the 3D CROW consisting of mode-gap cavities with modulation strength 1.5 and 2 calculated by FDTD (black dots), TB model (green line), and DM model (red line). In the 3D simulation, $h = 0.37a$ (h is the thickness of the slab) and $\epsilon = 10.04$.

$k \approx 0.13$ $(2\pi/R)$; it agrees satisfactorily with the fully 3D FDTD results [23]. In contrast, the result from the TB model is symmetric about $k = 0.5$ (π/R). The excellent match between our DM model and the FDTD data confirms that dispersion of the cavity quasi-modes is indeed the physical reason for the failure of the TB model to accurately describe photonic crystal CROWs.

In conclusion, the dispersion of a CROW composed of photonic crystal cavities cannot be described by the standard TB model due to the breakdown of completeness of the resonant modes. We show a new model, taking into account the dispersive property of the mode profile of the single cavity in a CROW structure. Our model describes the dispersion of the PhC CROW accurately without additional free parameters. Dispersion of the modes is inherent in all cavities. For racetrack resonators [2,24] and PhC cavities with resonances far away from the bandedge, such as L3 cavities [25], dispersion is negligible and shows no discernible effect on the dispersion of the related CROW structures. However, for shallow defect cavities, such as mode-gap cavities with small modulation strength and double-heterostructure cavities [26,27] with small lattice mismatch, the defect modes are close to the edge of the waveguide band, which makes the dispersive nature of the modes become pronounced. The dispersion of CROWs of such cavities has strong asymmetry. Thus, our theory will be useful for describing all devices based on coupling of shallow defect cavities, such as delay lines [10], optical memory [28], and $\mathcal{PT}$ symmetric diodes [29].

Funding. European Research Council (ERC) (279248); Nederlandse Organisatie voor Wetenschappelijk Onderzoek (Netherlands Organisation for Scientific Research).

Acknowledgment. The authors thank Henri Thyrrestrup, Ad Lagendijk, and Willem L. Vos for helpful discussions.

REFERENCES AND NOTES

1. A. Yariv, Y. Xu, R. K. Lee, and A. Scherer, Opt. Lett. **24**, 711 (1999).
2. F. Xia, L. Sekaric, and Y. Vlasov, Nat. Photonics **1**, 65 (2007).
3. M. J. Hartmann, F. G. S. L. Brandão, and M. B. Plenio, Laser Photon. Rev. **2**, 527 (2008).
4. M. F. Yanik and S. Fan, Phys. Rev. Lett. **92**, 083901 (2004).
5. M. Hafezi, S. Mittal, J. Fan, A. Migdall, and J. M. Taylor, Nat. Photonics **7**, 1001 (2013).
6. R. O. Umucalılar and I. Carusotto, Phys. Rev. A **84**, 1 (2011).
7. S. Longhi, Phys. Rev. E **75**, 1 (2007).
8. M. F. Yanik and S. Fan, Phys. Rev. Lett. **93**, 1 (2004).
9. E. Kuramochi, M. Notomi, S. Mitsugi, A. Shinya, T. Tanabe, and T. Watanabe, Appl. Phys. Lett. **88**, 1 (2006).
10. M. Notomi, E. Kuramochi, and T. Tanabe, Nat. Photonics **2**, 741 (2008).
11. N. Matsuda, E. Kuramochi, H. Takesue, and M. Notomi, Opt. Lett. **39**, 2290 (2014).
12. N. Ashcroft and N. Mermin, *Solid State Physics* (Saunders College, 1976).
13. P. Chak and J. E. Sipe, Opt. Lett. **31**, 2568 (2006).
14. M. Sumetsky and B. Eggleton, Opt. Express **11**, 381 (2003).
15. K. M. Leung and Y. F. Liu, Phys. Rev. B **41**, 10188 (1990).
16. A. Taflove and S. C. Hagness, *Computational Electrodynamics: The Finite-Difference Time-Domain Method*, 3rd ed. (Artech House, 2005).
17. A. F. Oskooi, D. Roundy, M. Ibanescu, P. Bermel, J. D. Joannopoulos, and S. G. Johnson, Comput. Phys. Commun. **181**, 687 (2010).
18. J. J. Sakurai, *Modern Quantum Mechanics* (Addison-Wesley, 1994).
19. E. Ching, P. Leung, A. Maassen van den Brink, W. Suen, S. Tong, and K. Young, Rev. Mod. Phys. **70**, 1545 (1998).
20. To decrease the time of the transient, the dielectric is made slightly lossy, given by $\epsilon(\omega) = \epsilon(\infty) + \frac{\sigma\omega_a^2}{\omega_a^2 - \omega^2 - i\omega\gamma_a}$, where $\omega_a = 5(2\pi c/a)$, $\gamma_a = 30(2\pi c/a)$, and $\sigma = 0.5$. The strength of this artificial loss has not influenced our results.
21. R. Faggiani, A. Baron, X. Zang, L. Lalouat, S. A. Schulz, K. Vynck, B. O. Regan, B. Cluzel, F. De Fornel, T. F. Krauss, and P. Lalanne, "Ultimate limits of light confinement in randomly-perturbed periodic structures," arXiv:1505.03472v1 (2015).
22. H. A. Haus and W. Huang, Proc. IEEE **79**, 1505 (1991).
23. The shape of the group velocity is independent of the resolution of the FDTD simulations. The absolute accuracy of the group velocity is estimated as 4%.
24. F. Xia, L. Sekaric, M. O'Boyle, and Y. Vlasov, Appl. Phys. Lett. **89**, 2004 (2006).
25. Y. Akahane, T. Asano, and B.-S. Song, Nature **425**, 944 (2003).
26. B.-S. Song, S. Noda, T. Asano, and Y. Akahane, Nat. Mater. **4**, 207 (2005).
27. J. Jágerská, N. Le Thomas, V. Zabelin, R. Houdré, W. Bogaerts, P. Dumon, and R. Baets, Opt. Lett. **34**, 359 (2009).
28. E. Kuramochi, K. Nozaki, A. Shinya, K. Takeda, T. Sato, S. Matsuo, H. Taniyama, H. Sumikura, and M. Notomi, Nat. Photonics **8**, 474 (2014).
29. H. Ramezani, H.-K. Li, Y. Wang, and X. Zhang, Phys. Rev. Lett. **113**, 263905 (2014).